Anal. Chem. **2007,** *79,* 494−499

Effect of Cluster Size in Kiloelectronvolt Cluster Bombardment of Solid Benzene

Edward J. Smiley, Nicholas Winograd, and Barbara J. Garrison*

Department of Chemistry, 104 Chemistry Building, The Pennsylvania State University, University Park, Pennsylvania 16802

Emission of benzene molecules by 5-keV cluster bombardment of a range of carbon projectiles from C_6H_6 to C_{180} is studied by a coarse-grained molecular dynamics (MD) technique. This approach permits calculations that are not feasible using more complicated potential energy functions, particularly as the interesting physics associated with the ion impact event approaches the mesoscale. These calculations show that the highest ejection yields are associated with clusters that deposit their incident energy 15−20 Å below the surface. The highest yield for the projectiles is produced by the C_{20} and C_{60} projectiles. The results from the MD simulations are also compared favorably to an analytical model based on fluid dynamics to describe the energy deposition. The analytical model is then utilized to extend the range of the calculations to higher incident energies. The issue of the relative amount of chemical fragmentation and intact molecular desorption is also examined for the benzene crystal. These results show that damage accumulation at high-incident fluence should not be problematic and that it should be possible to perform molecular depth profiling via secondary ion mass spectrometry experiments. In general, the approach presented here illustrates the power of combining a simplified MD method with analytical strategies for describing a length scale that is difficult to achieve with traditional MD calculations.

The availability of energetic (keV) cluster projectiles for the characterization and imaging of biomaterials[1,2] has created a need for a basic understanding of the physical phenomena associated with the impact event. In the experiment, a range of projectiles consisting of clusters with anywhere from two to millions of particles are utilized to desorb thermally labile molecules intact into a mass spectrometer.[3−7] Molecular dynamics (MD) computer simulations of the energy deposition event have traditionally been employed to follow the development of a collision cascade of atoms that ultimately lead to the desorption event.[8−10] With clusters, it has become clear in recent years, that the collective effects associated with the impact of multiple particles at essentially the same time give rise to larger scale motion including shock waves[11] and crater formation.[12−14] Although many simulations have been performed to model cluster bombardment using MD simulations, the substrates have been confined to simple materials like graphite,[15] silver,[13,14] silicon,[16] and thin layers of organics and water on metal substrates.[17,18]

For organic substrates, MD simulations can provide detailed information about the ion/solid interaction using atomic projectiles.[9] For example, not only is it possible to calculate the yield of molecules from a molecular solid, but it is also possible to gain some insight into bond-breaking and bond-forming events. These calculations are possible via the use of many-body interaction potentials such as the reactive empirical bond order (REBO) developed by Brenner and co-workers,[19] as well as with the extended version of this potential that includes long-range van der Waals-type interactions.[20] When employing these more sophisticated potential energy functions to cluster/surface collisions with more weakly bound solids such as benzene, the scale of the calculation quickly becomes intractable, since the energy dissipation extends over millions of substrate atoms and the computation time can exceed several months.[21]

* To whom correspondence should be addressed. E-mail: bjg@psu.edu.

(1) Winograd, N.; Postawa, Z.; Cheng, J.; Szakal, C.; Kozole, J.; Garrison, B. J. *Appl. Surf. Sci.* **2006**, *252*, 6836−6843.
(2) Cheng, J.; Winograd, N. *Anal. Chem.* **2005**, *77*, 3651−3659.
(3) Davies, N.; Weibel, D. E.; Blenkinsopp, P.; Lockyer, N.; Hill, R.; Vickerman, J. C. *Appl. Surf. Sci.* **2003**, *203*, 223−227.
(4) Weibel, D.; Wong, S.; Lockyer, N.; Blenkinsopp, P.; Hill, R.; Vickerman, J. C. *Anal. Chem.* **2003**, *75*, 1754−1764.
(5) Wong, S. C. C.; Hill, R.; Blenkinsopp, P.; Lockyer, N. P.; Weibel, D. E.; Vickerman, J. C. *Appl. Surf. Sci.* **2003**, *203*, 219−222.
(6) Rickman, R. D.; Verkhoturov, S. V.; Hager, G. J.; Schweikert, E. A. *Int. J. Mass Spectrom.* **2005**, *245*, 48−52.
(7) Takáts, Z.; Wiseman, J. M.; Gologan, B.; Cooks, R. G. *Science* **2004**, *306*, 471−473.
(8) Waldeer, K. T.; Urbassek, H. M. *Appl. Phys. A* **1988**, *45*, 207−215.
(9) Krantzman, K. D.; Postawa, Z.; Garrison, B. J.; Winograd, N.; Stuart, S. J.; Harrison, J. A. *Nucl. Instrum. Methods Phys. Res. Sect. B* **2001**, *180*, 159−163.
(10) Delcorte, A.; Bertrand, P.; Garrison, B. J. *J. Phys. Chem. B* **2001**, *105*, 9474−9486.
(11) Insepov, Z.; Yamada, I. *Nucl. Instrum. Methods Phys. Res. Sect. B* **1996**, *112*, 16−22.
(12) Aderjan, R.; Urbassek, H. M. *Nucl. Instrum. Methods Phys. Res. Sect. B* **2000**, *164*, 697−704.
(13) Postawa, Z.; Czerwinski, B.; Szewczyk, M.; Smiley, E. J.; Winograd, N.; Garrison, B. J. *J. Phys. Chem. B* **2004**, *108*, 7831−7838.
(14) Postawa, Z.; Czerwinski, B.; Szewczyk, M.; Smiley, E. J.; Winograd, N.; Garrison, B. J. *Anal. Chem.* **2003**, *75*, 4402−4407.
(15) Kerford, M.; Webb, R. P. *Nucl. Instrum. Methods Phys. Res. Sect. B* **2001**, *180*, 44−52.
(16) Krantzman, K. D.; Kingsbury, D. B.; Garrison, B. J. *Appl. Surf. Sci.* **2006**, *252*, 6419−6422.
(17) Postawa, Z.; Czerwinski, B.; Winograd, N.; Garrison, B. J. *J. Phys. Chem. B* **2005**, *109*, 11973−11979.
(18) Szakal, C.; Kozole, J.; Russo, M. F., Jr.; Garrison, B. J.; Winograd, N. *Phys. Rev. Lett.* **2006**, *96*, 216104.
(19) Brenner, D. W.; Shenderova, O. A.; Harrison, J. A.; Stuart, S. J.; Ni, B.; Sinnott, S. B. *J. Phys.: Condens. Matter* **2002**, *14*, 783−802.

10.1021/ac061531u CCC: $37.00
Published on Web 11/18/2006

To achieve meaningful MD simulations from the cluster bombardment of molecular solids, it is essential to choose which processes most critically influence the overall dynamics and which processes may be safely ignored. For benzene solid, the presence of the H atom is particularly problematic since its low mass requires most of the attention from the integration routines. In order to maintain the molecular structure and include bond fragmentation yet omit the costly H atom motion, the C−H fragment is considered a single particle. With this representation, there can be CH−CH bond cleavage, and thus, we can obtain some level of understanding how much fragmentation will occur. The coarse-graining (CG) method has been employed successfully in a number of situations where the molecular complexity demands this type of approximation.[22−25] To prove the efficacy of utilizing CG in this environment, we have already shown that the trajectory of molecular solid benzene containing only $(CH)_6$ and bombarded by 500-eV C_{60} projectiles does not change significantly when compared to full atomistic calculations. In addition, the calculations could be performed nearly 50 times faster.[21]

The focus of this study is to determine a number of experimental observables during the cluster bombardment of a molecular benzene crystal. The calculations are performed using C_6H_6, $C_{10}H_8$, C_{20}, C_{60}, C_{120}, and C_{180} as incident projectiles at 5-keV incident energy. These projectiles were chosen in order to provide a range of smaller and larger projectiles around the most common used projectile, C_{60}. The two smallest molecules (benzene and naphthalene) are planar ring structures, and the other four are fullerenes. Moreover, to examine the effect of only changing the projectile mass, related calculations were carried out by altering the mass of carbon from 12 to 6 amu and to 24 amu. The results show that the maximum sputtering yield of benzene molecules was achieved using C_{20} or C_{60} and that larger clusters do not provide larger yields. Examination of the probability of breaking C−C bonds also shows that bombardment by all of the projectiles leads to more molecular desorption than fragmentation, suggesting that molecular depth profiling[26,27] is feasible for this system. To extend the kinetic energy range of the incident projectile, we have enlisted the aid of a recently developed analytical model that treats the early stages of the energy deposition within the framework of fluid dynamics.[28] This model requires knowledge of the region where energy is deposited shortly after impact. By combining these two approaches, the calculations may be extended to 40-keV C_{60} bombardment to examine the basic nature of the energy deposition. Hence, from the results reported here, we show that, by using a few strategic approximations and an appropriate analytical model, the response of a molecular solid from bombardment with a range of cluster projectiles with varying kinetic energies is now possible.

COMPUTATIONAL DETAILS

The MD calculations used to model particle bombardment are described in detail elsewhere.[29] Briefly, Hamilton's equations of motion are integrated to determine the position and velocity of each atom as a function of time. The final positions and velocities are used to calculate quantities that can be compared to experimental data and to analyze microscopic motions.

In order to ensure that the dynamics are representative of the experimental conditions, the incident cluster projectile must have incident kinetic energy of several kiloelectronvolts. The computational challenge is to make the system sufficiently large to contain all the dynamic events yet at the same time be computationally tractable. For example, initial simulations using an atomic representation of benzene with a 500-eV C_{60} projectile, a 23 184-molecule sample that is 171 Å wide by 99 Å deep required 6 months of computer time to model.[21] Simulations of 5-keV C_{60} bombardment of water ice, a system with a similar binding energy to benzene, required a 300 Å wide by 16 Å deep sample and took 4 months of computer time to evaluate on identical computer hardware.[30,31] A sample of benzene comparable to the water system using an atomic representation and the complex AIREBO potential[20] would require CPU time of several years for each incident particle.

Recently, we have shown that the scattering of 500-eV C_{60} from benzene can be modeled using a CG representation of benzene.[21] With the same crystal size as the atomic representation of benzene, the CG model provides very similar trajectory information with a 45-fold improvement in computational time. The number of ejected particles and the visual representation of the bombarded crystal are sufficiently similar to allow the use of a coarse-grained representation for these studies of the bombardment of the molecular solid benzene by a number of different carbon projectiles.

The CG configuration of benzene is represented by six combined CH particles of 13 amu. The benzene molecule has the same hexagonal shape as found for atomistic benzene but does not explicitly include the hydrogen atoms. The forces among the CH particles are described by several potential energy functions delineated elsewhere.[21] Briefly, a Lennard-Jones potential is used to describe the intermolecular interaction between the CH−CH particles located on different molecules. A Morse potential describes the interaction of bonded CH particles. In addition, weak Morse potentials are used to describe the 1,3 and 1,4 interactions on the same benzene molecule. These potentials are necessary to include in the calculation when the molecule is fragmented due to energetic collisions, and the particles get too close together. The REBO potential is used to describe the C−C and C−H interactions within the carbon projectiles. Finally, a weak Lennard-Jones potential is used for the C and H atoms of the projectile and the CH particles of the coarse-grained benzene. This CG representation allows for C−C bond cleavage due to energetic collisions but does not account for recombination of radicals

(20) Hautman, J.; Klein, M. L. *J. Chem. Phys.* **1989**, *91*, 4994−5001.
(21) Marrink, S. J.; Mark, A. E. *J. Am. Chem. Soc.* **2003**, *125*, 11144−11145.
(22) Zhigilei, L. V.; Leveugle, E.; Garrison, B. J.; Yingling, Y. G.; Zeifman, M. I. *Chem. Rev.* **2003**, *103*, 321−347.
(23) Yingling, Y. G.; Garrison, B. J. *J. Phys. Chem. B* **2004**, *108*, 1815−1821.
(24) Stuart, S. J.; Tutein, A. B.; Harrison, J. A. *J. Chem. Phys.* **2000**, *112*, 6472−6486.
(25) Smiley, E. J.; Postawa, Z.; Wojciechowski, I. A.; Winograd, N.; Garrison, B. J. *Appl. Surf. Sci.* **2006**, *252*, 6436−6439.
(26) Gillen, G.; Roberson, S. *Rapid Commun. Mass Spectrom.* **1998**, *12*, 1303−1312.
(27) Cheng, J.; Wucher, A.; Winograd, N. *J. Phys. Chem. B* **2006**, *110*, 8329−8336.
(28) Jakas, M. M.; Bringa, E. M.; Johnson, R. E. *Phys. Rev. B* **2002**, *65*, 165425.
(29) Garrison, B. J. In *ToF-SIMS: Surface Analysis by Mass Spectrometry*; Vickerman, J. C., Briggs, D., Eds.; Surface Spectra: Manchester, 2001; pp 223−257.
(30) Wojciechowski, I. A.; Garrison, B. J. *J. Phys. Chem. A* **2006**, *110*, 1389−1392.
(31) Russo, M. R., Jr.; Wojciechowski, I. A.; Garrison, B. J. *Appl. Surf. Sci.* **2006**, *252*, 6423−6425.

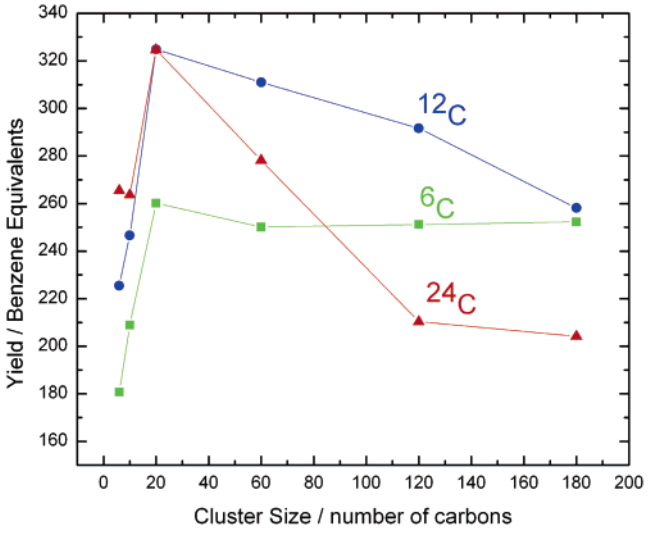

Figure 1. Total yield in benzene molecule equivalents as a function of cluster size for each of the six 5-keV carbon clusters and for each of the three carbon isotopes.

originating from different molecules.

The model approximating the benzene crystal consists of 198 720 benzene molecules arranged in 60 layers. Each layer consists of 3312 benzene molecules. The resulting crystal measures 341 Å × 341 Å × 207 Å in volume. Results from X-ray diffraction experiments show that the benzene crystal structure is orthorhombic with four molecules per unit cell.[32] In order to establish that the experimental configuration was stable within the CG description, the initial configuration of the crystal in an orthorhombic lattice is heated to 300 K, with a six-sided rigid boundary to prevent evaporation. The system is then quenched to 0 K using an algorithm based on the generalized Langevin equation.[33,34] The heating cycle does not destroy the orthorhombic crystal structure. The top two rigid layers are removed, and the crystal is relaxed at 0 K for 4 ps.

Previous simulations[14] indicate that each trajectory is nearly independent of impact point, and thus, only one trajectory is sampled for each of the six projectiles studied. Even with the CG representation, the simulation for each incident projectile requires 2 months of CPU time.[35] Each calculation of 27 ps begins with the projectile having 5 keV of kinetic energy bombarding the surface at normal incidence.

RESULTS AND DISCUSSION

The total sputtering yields for 5-keV C_6H_6, $C_{10}H_8$, C_{20}, C_{60}, C_{120}, and C_{180} bombardment of solid benzene are shown in Figure 1. For all clusters, the yields range from 180 to 325 equiv of benzene molecules and are large compared to those from atomic projectile bombardment. The results are also within the range of experimental yields for similar systems. The yields of ice[36] and trehalose[2] are 1820 water equivalents and 245 trehalose molecule equivalents, respectively, when bombarded by 20-keV C_{60}. Unpublished yields[37] of water ice as a function of C_{60} incident kinetic energy from 10 to 120 keV indicate that the yield increases linearly with incident energy, implying that the water ice yield at 5 keV should be between 400 and 500 molecule equivalents.

The trend in yield with cluster size is similar for all three carbon masses where a peak is observed for the C_{20} projectile. Each set of masses, however, has its own distinct characteristics. Aoki and Matsuo[38] as well as Anders and co-workers[39] see a similar overall trend in yield where the yield exhibits a maximum value for a cluster size of intermediate value while bombarding silicon[38] and Lennard-Jones solids,[39] respectively, using large argon clusters. Anders and Urbassek have predicted a mass-match effect for Lennard-Jones atomic systems.[40] Our results show that the trends established for atomic solids are also applicable to molecular targets. Of specific importance to the SIMS community in characterization of organic and biological samples is the prediction that, in general, the intermediate-sized ^{12}C clusters, i.e., C_{20} and C_{60}, give higher yields than clusters consisting of atoms with smaller and larger masses at 5-keV incident energy.

It would be valuable to relate the results of these detailed MD simulations to a simple analytical expression that allows a more direct estimate of the sputtering yields. Simulations of cluster bombardment indicate that it is essential to deposit the energy close to the surface.[41,42] Recently, Russo and Garrison have shown that the depth of energy deposition at a time when 90% of the energy is absorbed by the substrate is the critical parameter in determining the sputtering yield.[42] This observation led to the development of the mesoscale energy deposition footprint (MEDF) model, which is based upon the idea that the short-term behavior of cluster impact can be approximated by fluid dynamic flow and is described elsewhere.[42] In brief, after bombardment, an energy deposition track is created by the projectile. A volume of sputtered material is then determined by the width of the energy deposition footprint. Only atoms near the surface of this track can be displaced and escape toward the vacuum. If the energy is deposited too deep, then the energy is effectively wasted in terms of promoting ejection. From their correlations, then, they suggested that sputtering yields can be estimated from MD simulations carried out for just the first few hundred femtoseconds, greatly reducing the amount of required computer time.

To test this concept using the systems studied here, it is necessary to calculate, using MD, the projectile penetration depth when 90% of the initial kinetic energy is absorbed by the target. To acquire this number, the center of mass (COM) of the incident projectile is monitored as a function of time as it penetrates into the solid. Typical calculations of the COM depth for $^{12}C_6H_6$, $^{12}C_{60}$, and $^{12}C_{180}$ as a function of time are shown in Figure 2. As a means to show when the cluster dissociates, the one-dimensional radius of gyration of the cluster is shown as an error bar for each point.

(32) Cox, E. G. *Proc. R. Soc. London* **1932**, *A135*, 491−498.
(33) Garrison, B. J.; Kodali, P. B. S.; Srivastava, D. *Chem. Rev.* **1996**, *96*, 1327−1341.
(34) Adelman, S. A.; Doll, J. D. *J. Chem. Phys.* **1974**, *61*, 4242−4245.
(35) http://gears.aset.psu.edu/hpc/systems/lionxo/.
(36) Szakal, C.; Kozole, J.; Russo, M. F., Jr.; Garrison, B. J.; Winograd, N. *Phys. Rev. Lett.* **2006**, *96*, 216104.
(37) Szakal, C.; Kozole, J.; Winograd, N. Unpublished.
(38) Aoki, T.; Matsuo, J. *Nucl. Instrum. Methods Phys. Res. Sect. B* **2006**, *242*, 517−519.
(39) Anders, C.; Urbassek, H. M.; Johnson, R. E. *Phys. Rev. B* **2004**, *70*, 155404.
(40) Anders, C.; Urbassek, H. M. *Nucl. Instrum. Methods Phys. Res. Sect. B* **2005**, *228*, 57−63.
(41) Zimmermann, S.; Urbassek, H. M. *Nucl. Instrum. Methods B* **2005**, *228*, 75−83.
(42) Russo, M. R., Jr.; Garrison, B. J. *Anal. Chem.* **2006**, *78*, 7206.

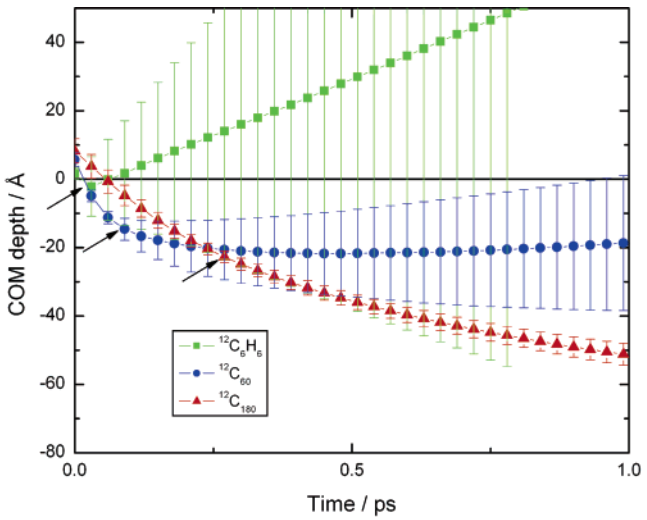

Figure 2. COM depth for 5-keV $^{12}C_6H_6$, $^{12}C_{60}$, and $^{12}C_{180}$ as a function of time. The black arrows indicate the time and depth at which 90% of the incident energy is deposited in the substrate. The bars in the vertical direction reflect the one-dimensional radius of gyration of the cluster at each point.

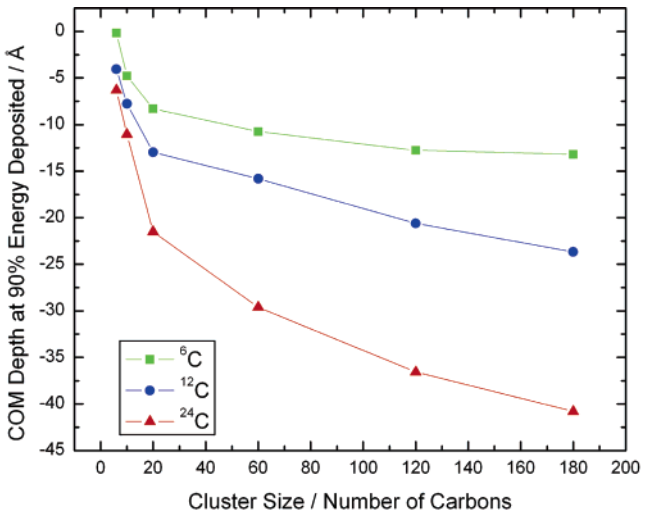

Figure 3. COM depth as a function of carbon cluster size when 90% of the incident 5 keV of energy is deposited. The figure is plotted with the depth in the negative direction with zero being the surface.

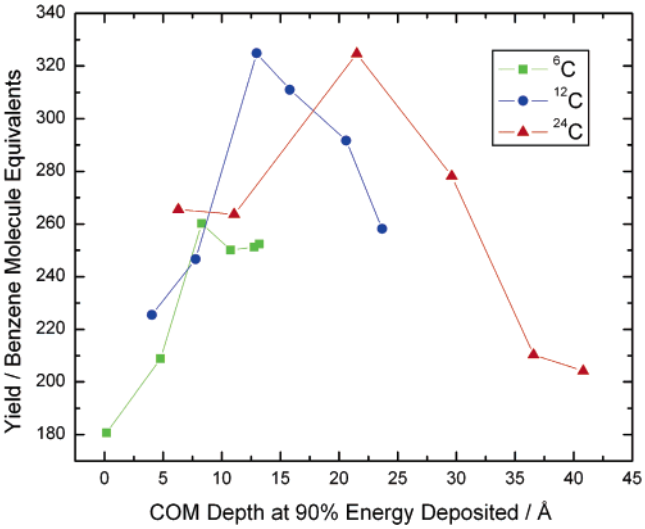

Figure 4. Total yield in benzene molecule equivalents as a function of COM depth when 90% of the initial 5 keV of kinetic energy has been deposited into the substrate. The colors indicate the same mass as in previous figures. The order of the points reflects the cluster size in numerical order.

For C_{60}, the initial radius of gyration is 2 Å in the direction perpendicular to the surface. For $^{12}C_6H_6$, the cluster impacts the benzene crystal and shatters almost instantly. The large radius of gyration indicates that some incident atoms are ejecting while others are penetrating into the solid. The $^{12}C_{60}$ projectile penetrates completely into the substrate with a deposition depth centered ~22 Å below the surface. Finally, the $^{12}C_{180}$ projectile is found to penetrate deeper into the substrate and it stays together much longer than the other two projectiles. For the $^{12}C_{180}$ cluster, the radius of gyration remains basically unchanged, indicating that all the atoms are at approximately the same depth although no information is implied about any spreading of the cluster in the lateral direction.

For the three projectiles shown in Figure 2, the corresponding times and depths when 90% of the energy is deposited are (28 fs, 4 Å), (107 fs, 16 Å), and (290 fs, 24 Å) for $^{12}C_6H_6$, $^{12}C_{60}$, and $^{12}C_{180}$, respectively. These depths are smaller and occur at much shorter times than the maximum penetration depth of the projectile. It is at this short time, however, that the fluidlike flow of the system can commence.[42] The COM depths for all projectiles at a time when 90% of the energy is deposited are shown in Figure 3. In this plot, a depth of zero indicates the surface of the substrate while negative numbers represent distances into the substrate. Two distinct mass trends can be observed. First, using the C_{60} cluster as an example, it is observed that the light mass $^{6}C_{60}$ penetrates the least and the heavy mass $^{24}C_{60}$ penetrates the most. Second, as the number of atoms increases, the penetration depth increases. These mass trends are key in understanding where the incident energy is placed in the substrate, which relates to the optimum depth of energy deposition.

The relationship of the sputtering yield to the COM depth when 90% of the energy is deposited is shown in Figure 4. There is a region from about 13 to 22 Å where the sputtering yields are at maximum, which is comparable to the value of 20 Å found for water−ice.[42] Clusters, such as all ^{6}C projectiles, that deposit their energy above the optimal depth are not fully using their energy for ejection events. As mentioned earlier, the yield of the ^{6}C projectiles levels off as the cluster size increases. The leveling off can be explained by the results presented in Figure 3, which shows that the depth for the ^{6}C clusters is very similar for all clusters from size 20 to 180. An opposite effect is observed for the projectiles with a COM penetration depth greater than 22 Å. Since the momentum of the projectile carries it deep into the surface, much of the energy is deposited too deep into the solid to allow it to be useful for sputtering. This type of energy deposition can be compared to heavy metal clusters, such as Au_3, which penetrates deeply into a water−ice target.[42] The key concept arising from this analysis is that these simulations support the prediction of the MEDF model of an optimum depth for energy deposition to maximize the yield.

Since there is a correlation of where the projectile energy is deposited and the total sputtering yield, it is instructive to analyze the important factors giving rise to the relative depths. For this analysis, there are two mass (momentum) effects to take into

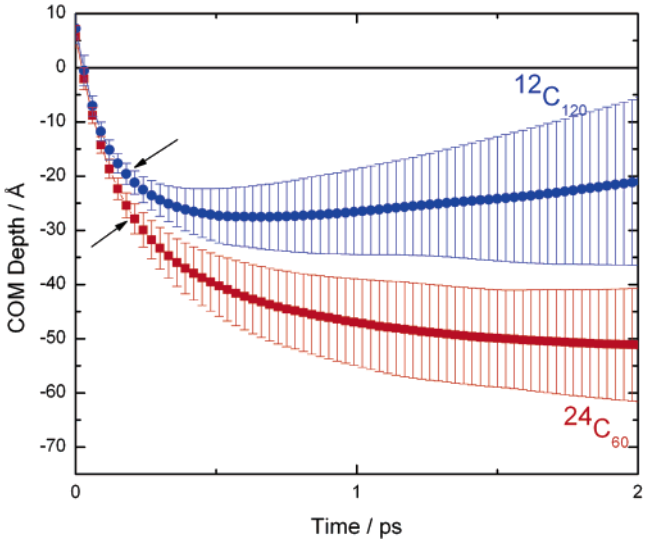

Figure 5. COM depth for 5-keV $^{24}C_{60}$ and $^{12}C_{120}$ as a function of time. The bars in the vertical direction reflect the one-dimensional radius of gyration of the cluster at each point.

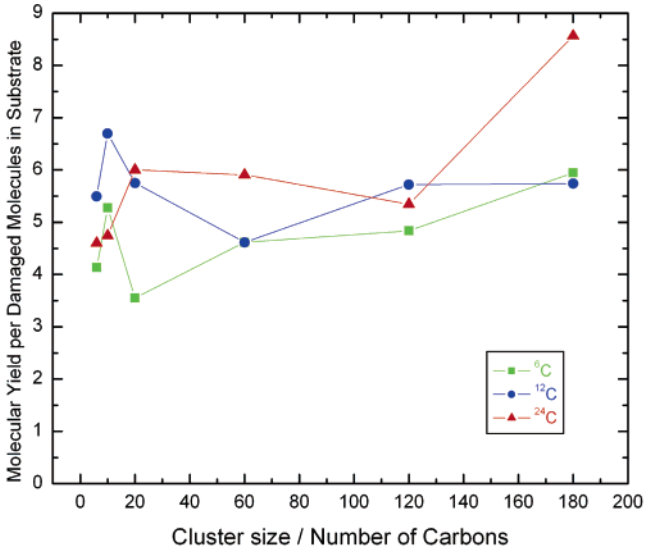

Figure 6. Ratio of the intact molecular yield of benzene molecules to the number of damaged benzene molecules left in the substrate.

account. First, there is the momentum of the total cluster, P_{tot}, of

$$P_{tot} = (2m_{tot}E)^{1/2} \quad (1)$$

where m_{tot} is the total mass and E is the energy of the cluster. As the total mass increases, the total momentum also increases; therefore, the projectile penetrates deeper into the substrate as shown in Figure 3 by a set of values for $^{6}C_{60}$, $^{12}C_{60}$, and $^{24}C_{60}$. A second mass effect can also be observed. Using the ^{12}C clusters as an example, the total momentum can be explained by the following equation

$$P_{tot} = (2nm_{ind}E)^{1/2} \quad (2)$$

where n is the number of carbon atoms in the cluster and m_{ind} is the mass of the individual carbon atom. As the number of carbon atoms in each cluster increases, the total momentum increases, and the penetration depth is greater for $^{12}C_{180}$ compared to $^{12}C_6H_6$.

Interplay of the two mass effects is observed when two different projectiles have the same total mass. An example is $^{12}C_{120}$ and $^{24}C_{60}$, which both have a mass of 1440 amu. Even though the total mass is the same, the actions of the clusters into the substrate are different as shown in Figure 5. At early times, both projectiles track with the same type of motion due to the fact that they are still intact and acting as one particle with the same total mass and same velocity. After the projectile starts to break apart, however, the individual mass effect becomes more influential, and the projectiles start acting like individual carbon atoms of mass 12 and 24 amu. The $^{12}C_{120}$ projectile is a better individual mass match for the benzene substrate. In this case, the substrate can absorb the impact from the projectile atoms more readily and start to reflect the energy. Since the mass of the individual carbon atom in $^{24}C_{60}$ is twice that of the CG particles in the benzene substrate, it penetrates deeper into the substrate. Similar effects have been reported in the past when C_{60} and Au_3 clusters impact water–ice[31] and argon substrates.[43]

An important application of cluster SIMS of organic solids is molecular depth profiling.[44–47] A key aspect is how much intact molecular ejection occurs relative to the number of damaged molecules left behind in the substrate.[26,27] The amount of damage caused by a projectile is important in revealing whether or not the projectile can be used for depth profiling experiments.[26,27] Since C–C bonds can be cleaved in this coarse-grained representation of benzene, it is possible to estimate the number of damaged molecules. Since only one trajectory was calculated for each projectile, there is too much statistical scatter to extract detailed trends as a function of cluster size. It is possible, however, to look at the damage to the substrate compared to how many intact molecules are sputtered. The ratio of the intact molecular yield to the number of damaged molecules left in the substrate is plotted in Figure 6 for all the projectiles. The ratios are consistently on the order of 4–6, and all values are larger than 3.5, showing conclusively that these projectiles are able to eject a large amount of intact molecular species and leave only a small amount of damage in the sample substrate.[26,27] Moreover, the large number of molecules ejected intact relative to the number of fragmented molecules indicates that our CG approximation of omitting CH bond breaks and radical–radical recombinations is sensible.

The MEDF model allows for the prediction of yields in short calculation times. The current study encompasses only a single projectile energy. Preliminary results are shown in Figure 7 for $^{12}C_{60}$ with kinetic energies of 5–40 keV run for only a short time. The maximum penetration depth for all projectiles at these energies is approximately the same. The depth at which 90% of the incident energy is deposited ranges between 15.7 Å for 5 keV to 18.5 Å for 40 keV with all values within the optimum depth.

(43) Anders, C.; Urbassek, H. M. *Nucl. Instrum. Methods Phys. Res. Sect. B* **2005**, *228*, 84–91.
(44) Mahoney, C. M.; Roberson, S. V.; Gillen, G. *Anal. Chem.* **2004**, *76*, 3199–3207.
(45) Wagner, M. S. *Anal. Chem.* **2004**, *76*, 1264–1272.
(46) Wagner, M. S. *Anal. Chem.* **2005**, *77*, 911–922.
(47) Szakal, C.; Sun, S.; Wucher, A.; Winograd, N. *Appl. Surf. Sci.* **2004**, *231–2*, 183–185.

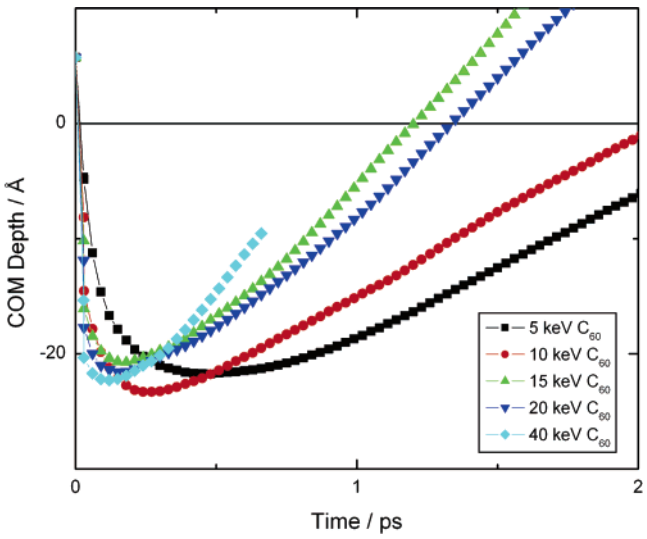

Figure 7. COM depth for 5−40-keV $^{12}C_{60}$ as a function of time. The 90% incident energy deposition occurs between 15.7 and 18.5 Å.

The MEDF model in conjunction with short-time simulations predicts that the yield should be approximately linear with increasing energy. This trend has been observed previously with extensive MD simulations of Lennard-Jones solids[35] and experimentally for C_{60} bombardment of water−ice.[37]

CONCLUSIONS

A series of molecular dynamics calculations of 5-keV bombardment of the molecular solid, benzene, by a series of projectiles from C_6 to C_{180} with three isotopes, including two artificial ones, ^6C, ^{12}C, and ^{24}C have been performed in order to understand the effect of cluster size and individual atom mass on yields. The ability to make such a series of calculations has been facilitated by using a coarse-grained representation for the benzene molecules. Several observations have arisen from these simulations. First, the predicted yield values are the same order of magnitude with experimental values on comparable systems and are large compared to atomic projectiles.[18,27] Second, for organic solids, the largest yields arise when the mass of the constituent atoms in the cluster projectile matches that of the target. Third, there is an intermediate cluster size that gives the largest molecular sputter yields. Fortunately for the experimentalists, this optimum mass and size is C_{20} or C_{60}. Fourth, the calculations show that, independent of cluster size or isotope mass, the ratio of sputtered intact molecules to the number of damaged molecules left in the solid is $\sim 5 \pm 1$, a promising situation for molecular depth profiling. Finally, we utilize the predictions of the analytic MEDF model to estimate yields after calculations extending to only a few hundred femtoseconds after impact. This strategy shows there is an optimal energy deposition depth and that MD calculations can be utilized at incident cluster energies up to 40 keV.

The ability to use a CG representation to model energy particle bombardment opens the door to model realistically sized systems for kiloelectronvolt particle bombardment. This simplification allows for the ability to look at damage to the substrate with less computer time. In addition, one is not limited to only the elements C and H as is the case for the AIREBO potential.

ACKNOWLEDGMENT

The financial support of the National Science Foundation through the Chemistry Division is gratefully acknowledged. Computational support was provided by the Graduate Education and Research Services (GEaRS) group at Penn State University. The authors acknowledge Zbigniew Postawa, Mike Russo, Kate Ryan, Christopher Szakal, and Andreas Wucher for insightful scientific conversations.

Received for review August 16, 2006. Accepted October 18, 2006.

AC061531U